AXON VOLTAGE-CLAMP SIMULATIONS

II. Double Sucrose-Gap Method

JOHN W. MOORE, FIDEL RAMÓN, *and* RONALD W. JOYNER

From the Department of Physiology and Pharmacology,
Duke University Medical Center, Durham, North Carolina 27710

ABSTRACT This is the second in a series of four papers on the simulation of the
voltage clamp of cylindrical excitable cells. In this paper we evaluate the double
sucrose-gap voltage-clamp technique for the squid and lobster giant axons. Using
the Crank-Nicolson method of solution of the cable equations and differential equa-
tions representing the voltage clamp circuit we studied the effect of length of the
sucrose gap "node" on the voltage profile along an excitable cell during a simulated
voltage clamp. The voltage gradients along the region of the cell within the node pro-
duce "notches" in the current recording as well as changes in the magnitude of the
sodium and potassium current for a given voltage step. Our results show that good
voltage clamp control requires node lengths less than one-half the axon diameter.

INTRODUCTION

In this paper we describe simulations to evaluate several arrangements where control
of the potential in an axon region is attempted by injection of current at a point and
where the membrane voltage is recorded at a point. Special emphasis is placed on the
study of the double sucrose gap (Julian, Moore, and Goldman, 1962 *a, b*). Neverthe-
less this type of voltage clamp simulations also applies to arrangements where separate
microelectrodes are used for current injection and voltage recording, or to a combina-
tion of a single sucrose gap with microelectrode recording.

In the original experiments we observed that current "notches" developed when the
length of the node exceeded the diameter. Lacking a quantitative evaluation of the
method, we used rough calculations and these experimental observations as a guide
in setting up the criterion that the length of the artificial node be short compared with
the axon diameter. The simulation methods described in the preceding paper (Moore
et al., 1975) now allow us to establish this criterion in a quantitative manner.

We now treat the normal (intact) axon as a truly distributed system. The three axon
clamp configurations which we have studied are shown in Fig. 1. They include: (*1*) cur-
rent and voltage electrodes placed at opposite ends of a cable (Fig. 1 A), simulating a
double sucrose gap; (*2*) voltage recording at one end with current injection at some
point near the center of the cable (Fig. 1 B), simulating an attempt to clamp a post-
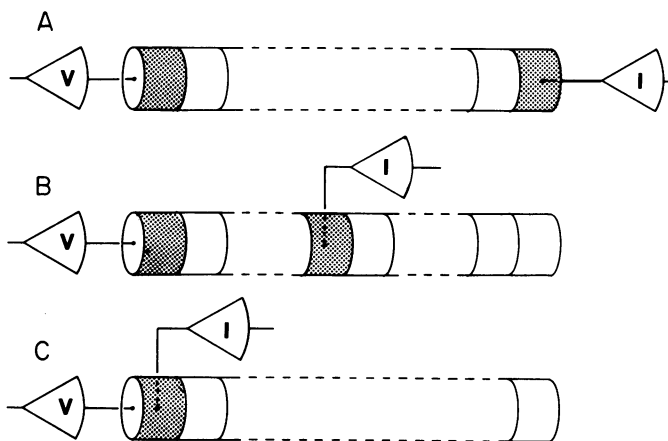synaptic region of axon; (*3*) both current and potential electrodes in the same segment

FIGURE 1 Schematic representation of several configurations of cables with varying position of the current injection and voltage recording electrodes which have been simulated. See text for further description.

(in this case, Fig. 1 C), at the same end of the cable, simulating a small spherical cell with an axon connected.

The voltage response of the individual cable segments are distinctive and will be described as appropriate under one of these configurations.

Current Injection and the Voltage Monitoring at Opposite Ends of Cable

In this situation which simulates a double sucrose gap, part of the access resistance is external to the cable and part is distributed along the interior (axoplasm) of the axon. The current injected supplied at one end of the cable required to control the potential at the other (monitored) end, causes a voltage gradient along the axon.

The original idea for the double sucrose-gap method of voltage clamp of non-myelinated fibers was to approach voltage uniformity by using an exposed artificial node which was short compared with the axon diameter. In order to quantitatively evaluate the quality of the sucrose-gap voltage clamp, the usual experimental conditions for squid and lobster axons were represented by approximately the same parameter values as previously used and given in Table II of the preceding paper (Moore et al., 1975). As before, the axoplasm resistivity was taken as 35.4 Ω-cm and the membrane was represented by the Hodgkin and Huxley (1952) model. As before, we scaled up the maximum conductance two-fold, taking $\bar{g}_{Na} = 240$ mmho/cm^2 and $\bar{g}_K = 72$ mmho/cm^2, à la FitzHugh and Cole (1964).

Simulations for a 500 μm "artificial node" in a squid axon 500 μm in diameter are shown in Fig. 2 A. The node is treated as 20 segments of 25 μm each, with the voltage electrode in segment 20 (R) and the current electrode in segment 1 (I). A 50 mV depolarizing potential step was chosen because it produces nearly the maximum transient sodium current and is in the negative resistance region where anomalous currents are most frequently observed. The upper part of the figure displays the potential across the
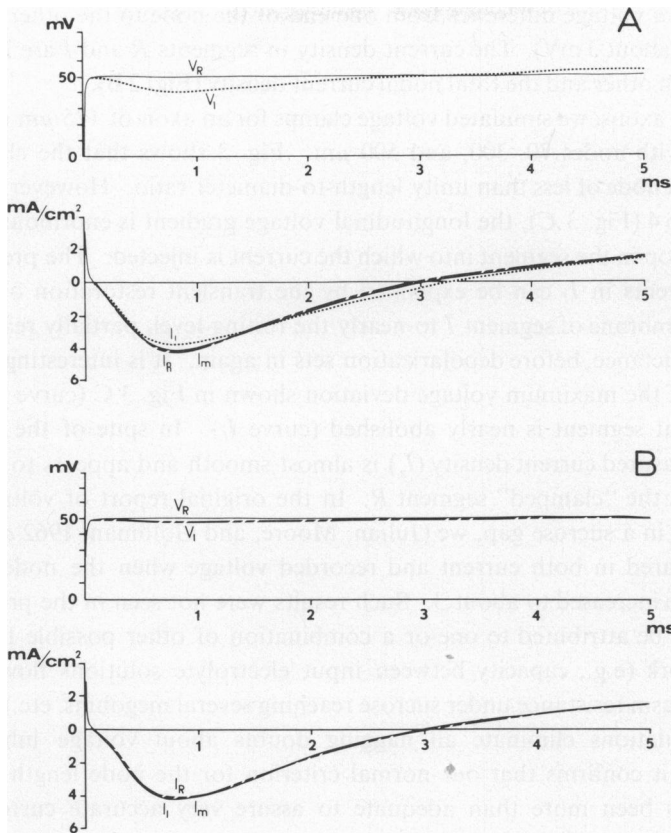
FIGURE 2 Results of simulation of a double sucrose-gap voltage-clamp for a squid axon of diameter 500 μm, using the configuration of Fig. 1 A with the current and voltage electrodes at opposite terminal segments. In part A the cable length is 500 μm, while in part B it is 250 μm. In both A and B, the upper records show the voltages at the end segments. In both A and B the lower records show the currents; the continuous line (barely seen on the current records) shows the total current density while the dotted and dashed lines represent the current densities of segments R and I, respectively. In part B, all current traces almost superimpose on one another.

membrane of the voltage recording segment (V_R) and at the current injection segment (V_I). It can be seen that for a node length equal to diameter which has been previously considered a "worst-case" condition the current injection segment (I) is nearly clamped and the voltage gradient along the node is only about 12 mV across the 500 μm. The lower part of the figure shows the current density from these two segments and that measured across the whole node (I_m). It is clear that the simulated measured current density from the whole node is very close to that in the well clamped segment R in spite of the clear departure of the current in segment I.

The criterion which we normally use in experiments is to adjust the node length to 1/2 or 1/4 of the diameter. Simulations of a node length of 250 μm (1/2 of the diame-

ter) results in a voltage difference from one end of the node to the other that is much smaller (only about 3 mV). The current density in segments R and I are indistinguishable from each other and the total nodal current density (Fig. 2 B).

For lobster axons, we simulated voltage clamps for an axon of 125 μm diameter in a sucrose gap with nodes 70, 300, and 500 μm. Fig. 3 shows that the clamp is again excellent for a node of less than unity length-to-diameter ratio. However, as this ratio is increased to 4 (Fig. 3 C), the longitudinal voltage gradient is enormous and current notches develop in the segment into which the current is injected. The presence of two transient currents in I_I can be explained by the transient restoration of the voltage across the membrane of segment I to nearly the resting level, partially reactivating the sodium conductance, before depolarization sets in again. It is interesting to note that at the time of the maximum voltage deviation shown in Fig. 3 C (curve V_I) the ionic current in that segment is nearly abolished (curve I_I). In spite of the notches, the simulated measured current density (I_s) is almost smooth and appears to be similar to the current in the "clamped" segment R. In the original report of voltage clamping lobster axons in a sucrose gap, we (Julian, Moore, and Goldman, 1962 a) found that notches appeared in both current and recorded voltage when the node's length-to-diameter ratio increased to about 3. Such results were not seen in the present simulations and can be attributed to one or a combination of other possible limitations of that early work (e.g., capacity between input electrolyte solutions flowing through tubing, axoplasm resistance under sucrose reaching several megohms, etc.).

These simulations eliminate all nagging doubts about voltage inhomogenities. Furthermore it confirms that our normal criterion for the node length (≤ 0.5 times diameter) has been more than adequate to assure very accurate current transient records.

It also follows that in the natural nodes in frog and *Xenopus* axons, where the node length and diameter are about equal, a good voltage uniformity can be achieved and the observed current is a good reflection of that for an ideal voltage clamp. It appears that, following dissection and manipulation of the fiber, the myelin gradually pulls back from the node during an experiment. Hille (1967) interprets the observed current changes to indicate that the newly exposed areas of membrane have a much lower density of sodium channels than does the natural nodal area. Thus the quality of the nodal clamp probably does not deteriorate as much with myelin retraction as might be expected if all of the membrane had a uniform and high density of sodium channels.

The double sucrose gap has been applied to smooth and cardiac muscle for purposes of voltage clamping (Anderson, 1969; Rougier et al., 1968). In these preparations where the fibers are 5–10 μm in diameter, it has not been possible to achieve artificial nodes which are less than several diameters. Therefore one can expect voltage clamp degradation in such preparations which are as bad or worse than those shown in Fig. 3 C for a long node in a lobster axon.

We can summarize the results obtained from the cables of different dimensions as follows: If a cable is "pulsed" with a family of rectangular pulses, the membrane volt-
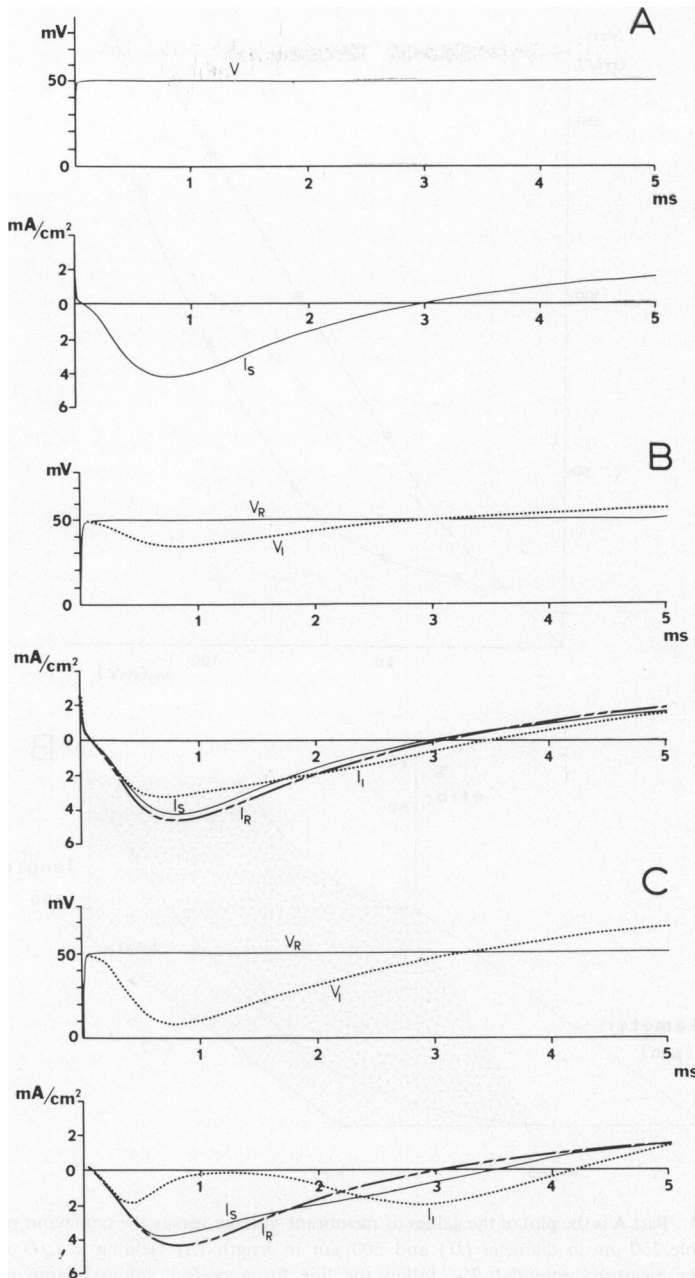
FIGURE 3   Results of simulation of the double sucrose-gap voltage clamp of the lobster axon of diameter 125 μm, using the configuration of Fig. 1 A with the voltage and current electrodes at opposite terminal ends.   In part A the length of the axon is 70 μm, in part B 300 μm, and in part C 500 μm.   In each part the voltages and currents at the two terminal segments are plotted along with the total ionic current.   For the voltage records (upper), the continuous line represents the voltage across segment R (V_R) and the dotted line the voltage across segment I (V_I).   For the current traces (lower) the continuous line shows the total current (I_s), the dotted line the current through segment I (I_I) and the interrupted line the current at segment R (I_R). In part A all current records superimpose.

29
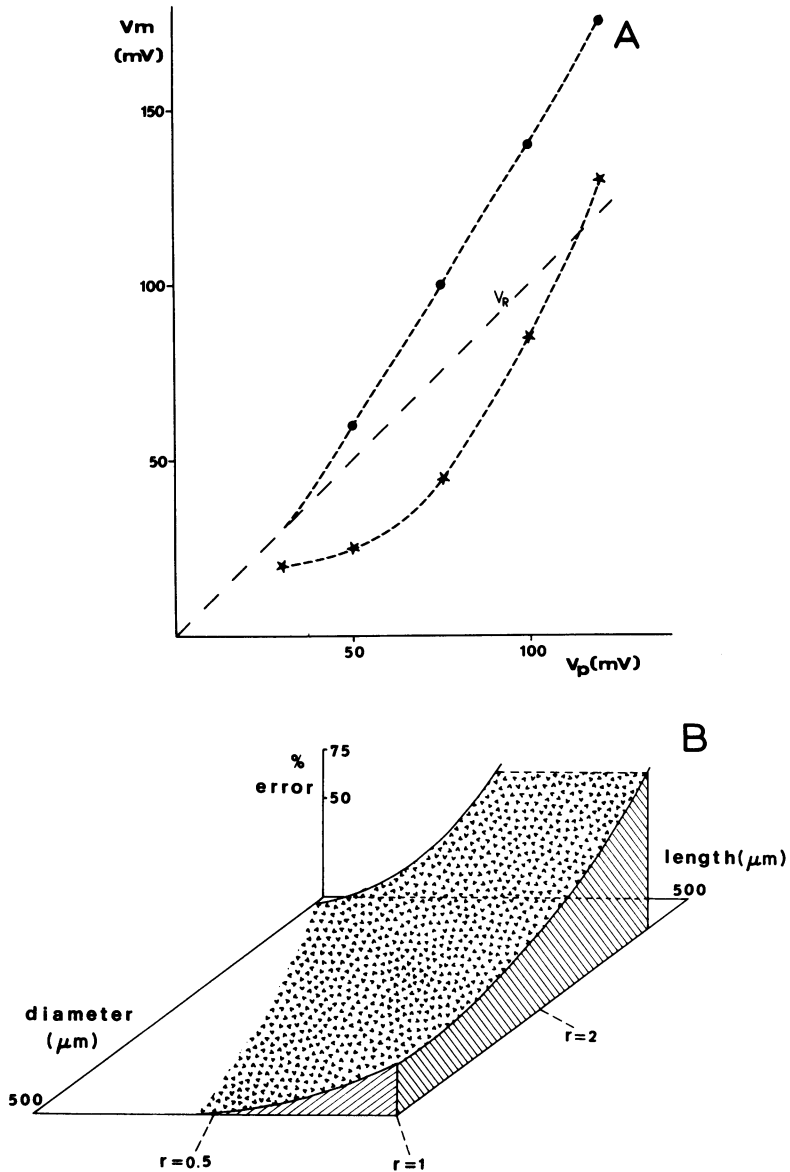
FIGURE 4   Part A is the plot of the values of membrane voltage versus the command pulse taking for a cable 250 μm in diameter (D) and 500 μm in length (L) yielding a L/D ratio equal to 2. The measured potential, V_R, follow the line for a perfect voltage clamp drawn at a 45° angle. The maximum departures from this potential occur in the current injection segment. The stars show the maximum deviation of the transmembrane voltage during the transient conductance phase and the circles show the steady-state deviations. Note that the maximum transient deviation of the transmembrane voltage from the command potential, (50%) occurs for a 65 mV depolarizing step. Part B is a three-dimensional plot of the maximum errors of the transmembrane voltage, as a percentage of the command pulse value, during the transient current. The data for the plot was obtained as shown in part A and are plotted versus the length and the diameter of the cable for a number of combinations. For reference, three lines showing L/D ratios of 0.5, 1.0, and 2.0 are also drawn.

age of the patch being recorded (V_R) follows the command pulse, while the membrane voltage of the patch where current is being injected V_I deviates from it. When V_R is plotted versus the command potential, the result is a straight line with slope of 1 (Fig. 4 A) at all potential steps. The maximum departures from this value occur in the current injection segment. The stars indicate this departure during the transient current and the circles during the steady state. For command potentials below the sodium equilibrium potential the transient deviation is in the hyperpolarizing direction and in the depolarizing direction for command potentials above the sodium equilibrium potential.

In order to effectively summarize the contribution of the various parameters, they are presented in a three-dimensional plot in Fig. 4 B, where the ordinate is the maximum deviation of the ratio of the membrane potential to the control potential. The cable parameters chosen were the diameter and the length between the two electrodes.[1] For reference, three ratios of cable length to diameter are shown. The voltage across the membrane deviated at the current injecting point by about 20% of the command pulse when the cable length is the same as the diameter (a ratio of 1) and more than 50% for ratios greater than 2. Voltage deviations of approximately 70% give rise to noticeable notches in the current records.

It is worth noting that, in the cable portion between the electrodes, during the phase of inward current, all voltage deviations are in the repolarizing direction. The deviations are produced by the control amplifier supplying the appropriate current for the clamped segment. Their effect in partially repolarizing some segments of the membrane to partially reactivate the sodium conductance leads to the notches. Depolarizing voltage deviations such as full or partial action potentials, cannot occur in these cable segments during this time.

Current Injection Near Center of Axon and Conditions in Extrapolar Cable Segments

In some cases, such as those illustrated in Fig. 1 B and 1 C, there is a portion of the axon that is not between the current and voltage electrodes and therefore is not in the feedback loop of the control amplifier. If the length of this region is equal to or less than the region in the feedback loop (interpolar), it will behave similarly to that portion for reasons of symmetry. When the region is longer than the interpolar region, its behavior is different and is described by the following results.

For the configurations shown in Fig. 1 B and 1 C, the current injected by the control amplifier causes depolarization to spread symmetrically along the cable for short distances in both directions. The cable region outside the feedback loop is free to propa-

---

[1]The error observed at the end of the cable as the deviation in voltage from the command pulse, has an unknown functional dependance on L/D. It might seem that this function should be $L/\sqrt{D}$, because the characteristic "length constant" is proportional to $\sqrt{D}$; ($\lambda = (D\ R_m/4R_i)^{1/2}$). However, the term "length constant" can apply only to the case of a passive cable and not to an active fiber, particularly under the "voltage-clamp" conditions studied in this series of papers. Therefore we will merely note this possible dependence in passing and we will describe the error in voltage in terms of the simple function L/D.
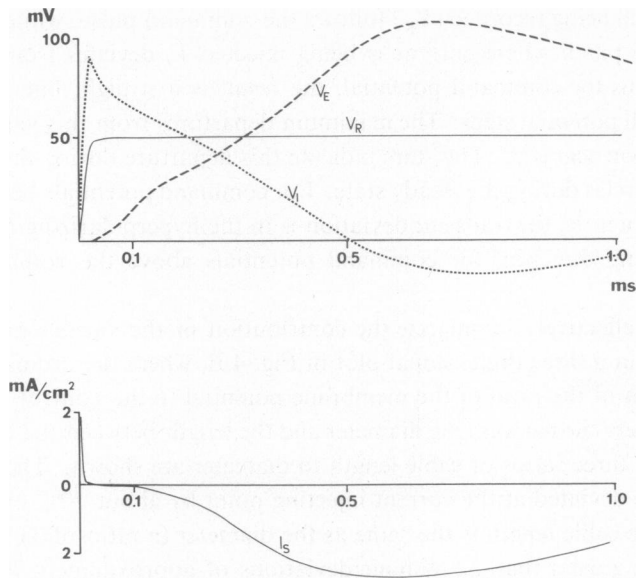
FIGURE 5 Simulation of the "voltage clamp" of a lobster axon 125 μm in diameter and 2 mm long. The configuration used was similar to that shown in Fig. 1 B, with the voltage recording segment (*R*) at the left end and current injected into the center segment (*I*). The segments to the right of *I* are not in the feedback loop. The upper graph shows the transmembrane potential pattern in the segments at the left (V_R), central (V_I), and right (V_E) ends of the axon. The total simulated ionic current density is shown in the lower graph.

gate an action potential if the depolarization reaches the membrane threshold. Fig. 5 shows the results of a computation using the configuration illustrated in Fig. 1 B. It can be seen that, while the membrane segment at the voltage sensing electrode (V_R) is voltage clamped and the patch where current is injected (V_I) follows the pattern described in the preceding section, the equidistant extrapolar region (V_E) of the cable experiences a propagated action potential.

The current produced by the membrane during a propagated action potential is very much smaller than that of a clamped patch. Therefore the current records are not significantly altered by the presence of an action potential. Extrapolar regions between the current injection point and the propagated action potential contribute small currents that follow approximately the same time course as those in the feedback loop.

The total membrane current, labeled "I_s," in Fig. 5 is similar to that of a clamped isopotential segment. It is important to notice that in this case, regardless of the length of the extrapolar region there are no notches in the current records. The general pattern of the current records is very similar to that of a clamped patch with small differences in the time course.

A clear example of the voltage inhomogeneity of this cable is shown in Fig. 6. The cable and conditions used for this computation are the same as those for Fig. 5 except that in this case the pulse was turned off at 0.5 ms (during the transient current). It can
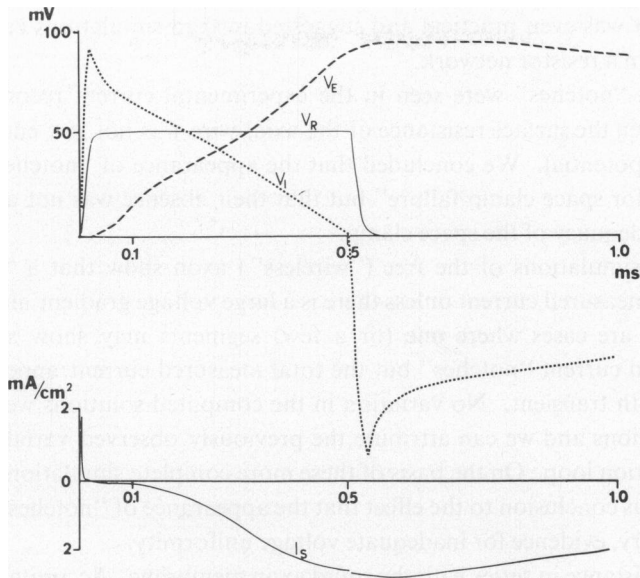
FIGURE 6 Simulation of a "voltage clamp" of the same cable used for Fig. 5. In this case, the command pulse was turned off at 0.5 ms, and the transmembrane voltage at left end (V_R) returns to zero almost immediately, while the transmembrane voltage at right end still goes through an action potential. Note however that the ionic current from the cable (I_s) is very similar to that of Fig. 5.

be seen that the current record does not show the normal exponential decay after the control pulse is turned off, but actually increases for some time before slowly declining. This anomalous result might be misinterpreted as a conductance change that, once turned on, goes through its normal course more or less independently of the new voltage levels.

If the voltage and current electrodes are reversed from the configuration shown in Fig. 5, the new configuration corresponds to the single sucrose-gap voltage-clamp technique (Kootsey and Johnson, 1972).

DISCUSSION

This work represents a much more realistic and extended evaluation of errors in the voltage clamp method which one of us considered more than a decade ago (Taylor, Moore, and Cole, 1960). Then we used a very much oversimplified "two patch model" for an axon skewered on an axial wire. The two patches were separated by an internal resistance and represent just two segments along the full cable considered in the present analysis. The solutions obtained frequently varied from run to run on the computer, giving strikingly different results for conditions in which current notches could occur. We were not sure whether this could be fully attributed to noise in the computation loop or whether it might be an inherent property of the H-H equations. At that time, we expressed the need for analysis of the complete, continuous model but were dubious

as to whether it was even practical and suggested instead simulations employing electronic analogs in a resistor network.

In that work "notches" were seen in the experimental current records and in the simulations when the surface resistance of the axial wire was not low enough to maintain a uniform potential. We concluded that the appearance of "notches" was "sufficient evidence for space clamp failure" but that their absence was not a sufficient criterion for the adequacy of the space clamp.

Our present simulations of the free ("wireless") axon show that a "notch" never appears in the measured current unless there is a large voltage gradient along the cable. However there are cases where one (or a few) segments may show strong voltage fluctuations and current "notches" but the total measured current appears to have a relatively smooth transient. No variation in the computed solutions were seen in the present simulations and we can attribute the previously observed variability to noise in the computation loop. On the basis of these more complete simulations we can confirm the previous conclusion to the effect that the appearance of "notches" is sufficient, but not necessary, evidence for inadequate voltage uniformity.

There is a resistance in series with the squid axon membrane. Accurate measurement of its magnitude requires very fast electronic circuits. The original value observed by Hodgkin et al. (1952) was 7 Ω-cm^2 but later estimates have ranged from 1 to 3 Ω-cm^2 (e.g., Cole and Moore, 1960). We have also considered the effect of this factor in our simulations evaluating the quality of the voltage clamp and treat it in some detail in the fourth paper of this series. For our present purposes we can summarize the observations applicable to the cases considered so far. Taking 7 Ω-cm^2 as the worst case for our squid axon simulation, we found that this resistance in series with the membrane does not drastically change the positive slope conductances of the peak and steady-state currents but it does shift the potential of the peak transient current and changes the negative slope markedly. Furthermore it introduces considerable distortion in the time course of the currents in this region. These results compare very well with experimental observations on the effect of altering this series resistance (e.g., Taylor et al., 1960). From this we can conclude that experiments designed for careful analysis of the peak magnitude of kinetics of the sodium conductance require appropriate compensation for the series resistance. For rough or comparative evaluations of the peak amplitude (e.g. in pharmacological studies) compensation may be omitted if great caution is exercised in interpretation of results.

REFERENCES

ANDERSON, N. 1969. *J. Gen. Physiol.* **54**:145.

COLE, K. S., and J. W. MOORE. 1960. *J. Gen. Physiol.* **44**:123.

FITZHUGH, R., and K. S. COLE. 1964. *Biophys. J.* **4**:257.

HODGKIN, A. L., A. F. HUXLEY, and B. KATZ. 1952. *J. Physiol. (Lond.).* **116**:424.

HODGKIN, A. L., and A. F. HUXLEY. 1952. *J. Physiol. (Lond.).* **117**:500.

HILLE, B. 1967. *J. Gen. Physiol.* **50**:1287.

JULIAN, F. J., J. W. MOORE, and D. E. GOLDMAN. 1962 *a*. *J. Gen. Physiol.* **45**:1195.

JULIAN, F. J., J. W. MOORE, and D. E. GOLDMAN. 1962 *b*. *J. Gen. Physiol.* **45**:1217.

KOOTSEY, J. M., and E. A. JOHNSON. 1972. *Biophys. J.* **12**:1496.

MOORE, J. W., F. RAMÓN, and R. JOYNER. 1975. *Biophys. J.* **15**:11.

ROUGIER, O., G. VASSORT, and R. STÄMPFLI. 1968. *Pfluegers Arch. Eur. J. Physiol.* **301**:91.

TAYLOR, R. E., J. W. MOORE, and K. S. COLE. 1960. *Biophys. J.* **1**:161.